Letter

Near-threshold resonances in ^{11}C and the ^{10}B$(p, \alpha)^7$Be aneutronic reaction

J. Okołowicz,[1] M. Płoszajczak [2] and W. Nazarewicz [3]

[1]*Institute of Nuclear Physics, Polish Academy of Sciences, Radzikowskiego 152, PL-31342 Kraków, Poland*
[2]*Grand Accélérateur National d'Ions Lourds (GANIL), CEA/DSM - CNRS/IN2P3, BP 55027, F-14076 Caen Cedex, France*
[3]*Facility for Rare Isotope Beams and Department of Physics and Astronomy, Michigan State University, East Lansing, Michigan 48824, USA*

The nucleus ^{11}C plays an important role in the boron-proton fusion reactor environment as a catalyzer of the ^{10}B$(p, \alpha)^7$Be reaction which, by producing a long-lived isotope of ^{7}Be, poisons the aneutronic fusion process ^{11}B$(p, 2\alpha)^4$He. The low-energy cross section of ^{10}B$(p, \alpha)^7$Be depends on the near-threshold states $7/2_1^+, 5/2_2^+, 5/2_3^+$ in ^{11}C whose properties are primarily known from the indirect measurements. In this work, we present the theoretical analysis of these resonances and their collectivization via the coupling to the proton emission threshold. By using the shell model embedded in the continuum, we show that a significant collectivization takes place that enhances the spectroscopic factor of proton capture confirming the phenomenological value of Wiescher *et al.* [Phys. Rev. C **95**, 044617 (2017)].

Introduction. Aneutronic plasma fusion reactions have been considered as possible energy sources that would avoid the disadvantage of producing neutron radiation and long-lived unwanted radioactive isotopes. Among the aneutronic energy sources, one finds ^{11}B$(p, 2\alpha)^4$He exothermic reaction with a Q value of 8.7 MeV, which does not produce any long-lived radioactive products. However, the natural boron fuel contains ^{10}B isotope whose abundance amounts to 19%, and which produces the long-lived radioactive ^{7}Be through a reaction ^{10}B$(p, \alpha)^7$Be that is poisoning the aneutronic energy source. The cross section for ^{10}B$(p, \alpha)^7$Be and the structural information about the near-threshold resonances in ^{11}C are known from the indirect Trojan horse method measurements [1–3] which have large model dependent uncertainties [3]. Extrapolations of the higher-energy R-matrix results to low energies suffer from the inconsistent experimental data and the lack of the reliable information on low-energy resonances [4]. Hence, the consistent analysis of the proton resonances in ^{11}C in the vicinity of the proton-decay threshold resonances is desired.

There are numerous examples of narrow resonances in light nuclei that can be found in the proximity of particle decay thresholds. Probably the most famous resonance of this kind is the excited 0_2^+ Hoyle state of ^{12}C very close to the α-particle separation energy, but numerous examples have been also found in exotic nuclei, e.g., in ^{11}Li [5], ^{11}B [6–11], ^{12}Be [12], ^{13}F [13], ^{15}F [14,15], ^{16}F [16], ^{14}O [17], and ^{26}O [18], generating a considerable interest in the formation mechanism of near-threshold resonances. In a model based on the R-matrix theory, Barker found an increased density of levels with large reduced widths near thresholds [19]. Based on studies in the shell model embedded in the continuum (SMEC) [20], it has been conjectured [5,21] that the coupling to the

decay channel(s) leads to a new kind of near-threshold collectivity, which may result in a formation of a single 'aligned eigenstate' of the system carrying many characteristics of a nearby decay channel. This mechanism provides a general explanation, based on the configuration mixing approach to open quantum systems, of the widespread appearance of cluster or correlated states in the vicinity of the cluster emission thresholds. Moreover, this mechanism is fairly independent of details of the interaction and the considered model space.

An unusual process, a β^--delayed proton decay of a halo nucleus ^{11}Be [22–24] was studied in Refs. [6–11,25]. The unexpectedly high strength of this decay mode was explained [25] by the presence of a narrow resonance in ^{11}B, recently found slightly above the proton separation energy [6–9]. In this Letter, we will discuss a possible collectivization of resonances in the proximity of a proton emission threshold in the mirror nucleus ^{11}C. The continuum-coupling-induced collectivization of these resonances and, hence, formation of the aligned states with large proton spectroscopic factors, may have an appreciable impact on the near-threshold cross section of the reaction ^{10}B$(p, \alpha)^7$Be. Moreover, more precise information about these resonances is important for improving R-matrix extrapolations of the data obtained at higher energies.

SMEC picture. In a simplest version of the SMEC, the Hilbert space is divided into two orthogonal subspaces $\mathcal{Q}_0$ and $\mathcal{Q}_1$ containing 0 and 1 particles in the scattering continuum, respectively. An open quantum system description of $\mathcal{Q}_0$ includes couplings to the environment of decay channels through the energy-dependent effective Hamiltonian

$$\mathcal{H}(E) = H_{\mathcal{Q}_0\mathcal{Q}_0} + W_{\mathcal{Q}_0\mathcal{Q}_0}(E), \qquad (1)$$

where $H_{Q_0 Q_0}$ denotes the standard shell model (SM) Hamiltonian describing the internal dynamics in the closed quantum system approximation, and

$$W_{Q_0 Q_0}(E) = H_{Q_0 Q_1} G_{Q_1}^{(+)}(E) H_{Q_1 Q_0} \qquad (2)$$

is the energy-dependent continuum coupling term, where E is the scattering energy, $G_{Q_1}^{(+)}(E)$ is the one-nucleon Green's function, and H_{Q_0, Q_1} and $H_{Q_1 Q_0}$ couple the subspaces Q_0 with Q_1. The energy scale in Eq. (1) is defined by the lowest one-nucleon emission threshold. The channel state is defined by the coupling of one nucleon in the scattering continuum to the SM wave function of the nucleus $(A - 1)$.

As in our previous SMEC studies of the mirror nucleus ^{11}B [10,11], for $H_{Q_0 Q_0}$ we take the Warburton-Brown Potential (WBP)-Hamiltonian [26] defined in the (psd) model space. The continuum-coupling interaction is assumed to be the Wigner-Bartlett contact force

$$V_{12} = V_0 [\alpha + \beta P_{12}^\sigma] \delta(\mathbf{r}_1 - \mathbf{r}_2), \qquad (3)$$

where $\alpha + \beta = 1$, P_{12}^σ is the spin exchange operator. For the spin-exchange parameter we take the standard value $\alpha = 0.73$ [20,27]. The radial single-particle wave functions (in Q_0) and the scattering wave functions (in Q_1) are generated by the average potential which includes the central Woods-Saxon term, the spin-orbit term, and the Coulomb potential. The radius and diffuseness of the Woods-Saxon and spin-orbit potentials are $R_0 = 1.27 A^{1/3}$ fm and $a = 0.67$ fm, respectively. The strength of the spin-orbit potential is $V_{SO} = 6.7$ MeV for protons and 7.62 MeV for neutrons, and the Coulomb part is calculated for an uniformly charged sphere with the radius R_0.

The SMEC eigenstates $|\Psi_\alpha^{J^\pi}\rangle$ of $\mathcal{H}(E)$ are the linear combinations of SM eigenstates $|\Phi_i^{J^\pi}\rangle$ of $H_{Q_0 Q_0}$. For a given total angular momentum J and parity π, the mixing of SM states in a given SMEC eigenstate $|\Psi_\alpha^{J^\pi}\rangle$ is due to their coupling to the same one-proton decay channel (ℓj). The continuum-induced mixing of SM states can be studied using the continuum-coupling correlation energy [10,11]

$$E_{\text{corr};\alpha}^{J^\pi}(E) = \langle \Psi_\alpha^{J^\pi}(E)|W_{Q_0 Q_0}(E)|\Psi_\alpha^{J^\pi}(E)\rangle. \qquad (4)$$

In this expression, for a given energy E, one selects the eigenstate $|\Psi_\alpha^{J^\pi}(E)\rangle$, which has the correct one-nucleon asymptotic behavior. For that, the depth of the average potential is chosen to yield the single-particle energy equal to E. The point of the strongest collectivization corresponds to the minimum of the correlation energy.

Results. The SMEC calculations for ^{11}C were carried out for a state $J^\pi = 7/2_1^+$ which is bound by 40 keV with respect to the proton-decay threshold, and two resonances $J^\pi = 5/2_2^+$, $5/2_3^+$ which are unbound by 10 keV and 510 keV, respectively [28], see Fig. 1. In the coupling to one-proton channels: $[^{10}B(3^+) \otimes p(s_{1/2})]^{J^+}$, $[^{10}B(3^+) \otimes p(d_{5/2})]^{J^+}$, $[^{10}B(3^+) \otimes p(d_{3/2})]^{J^+}$, the depth of Woods-Saxon potential for protons is chosen to yield proton single-particle state in $s_{1/2}$, $d_{5/2}$, and $d_{3/2}$ channels at the proton energy E_p. For the neutrons, the depth of Woods-Saxon potential is adjusted to reproduce the measured separation energy of the $p_{3/2}$ orbit.

The results presented in this work were obtained in four variants of calculations labeled by the index k. The
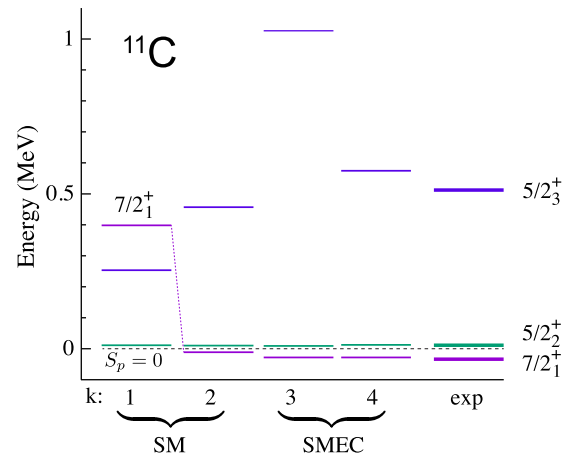

FIG. 1. Energies of $7/2_1^+$, $5/2_2^+$, and $5/2_3^+$ states in ^{11}C relative to the proton emission threshold (marked by a dashed line). Experimental data are taken from Ref. [28]. Various variants of SM and SMEC calculations are labeled by the index k. See text for details.

index $k = 1$ denotes SM calculations using the WBP-interaction [26] with the monopole terms $\mathcal{M}^{T=1}(0p_{1/2}, 1s_{1/2})$, $\mathcal{M}^{T=1}(0p_{1/2}, d_{5/2})$ shifted by -2.292 MeV and $+1$ MeV, respectively, as in the case of ^{11}B [10,11]. The SM variant $k = 2$ corresponds to the monopole shifts reduced by 50% compared to the $k = 1$ case. The variant $k = 3$ corresponds to SMEC calculations using the same SM interaction as in $k = 1$ but with the continuum coupling constant $V_0 = -430$ MeV fm^3. Finally, the SMEC variant $k = 4$ uses the $k = 2$ SM interaction and $V_0 = -150$ MeV fm^3. All considered resonances decay predominantly by the α-particle emission. For example, the proton single particle width of $5/2_2^+$ resonance is tiny, $\Gamma_p^{\text{s.p.}} = 2 \times 10^{-13}$ keV, as compared to the total experimental width of $\Gamma \approx 15$ keV [29]. In the SMEC calculation, the width of the $5/2_2^+$ resonance varies from 1.6×10^{-13} keV for $k = 3$ to 2.2×10^{-14} keV for $k = 4$. The energies of $7/2_1^+$, $5/2_2^+$, and $5/2_3^+$ states in ^{11}C obtained in all these calculation variants are shown in Fig. 1. It is seen that the standard SM interaction ($k = 1$) predicts the incorrect order of states, with the $7/2_1^+$ level shifted above $5/2_2^+$ and $5/2_3^+$ resonances. The $k = 2$ and $k = 4$ variants provide a very reasonable reproduction of measured energy levels.

Figure 2(a) shows the real part of the continuum-coupling correlation energy E_{corr} relative to V_0^2 for a weakly bound $7/2_1^+$ state of ^{11}C as a function of E_p. Away from regions of avoided crossing of SMEC eigenstates, and in the one-channel case, $E_{\text{corr}}/V_0^2(E_p)$ is a universal function of energy, independent of the continuum-coupling constant V_0.

One can see that the continuum-coupling correlation energy of $7/2_1^+$ is large, though the minimum of E_{corr} is not close to the experimental energy of this state. The dominant contribution to E_{corr} comes from the coupling to the channel $[^{10}B(3^+) \otimes p(d_{5/2})]^{7/2^+}$ but the contribution of the $\ell = 0$ channel $[^{10}B(3^+) \otimes p(s_{1/2})]^{7/2^+}$ is important as well, especially at near-threshold energies. The contribution from the channel $[^{10}B(3^+) \otimes p(d_{3/2})]^{7/2^+}$ is insignificant. The unusual pattern of E_{corr} seen in Fig. 2(a) can be explained in terms of
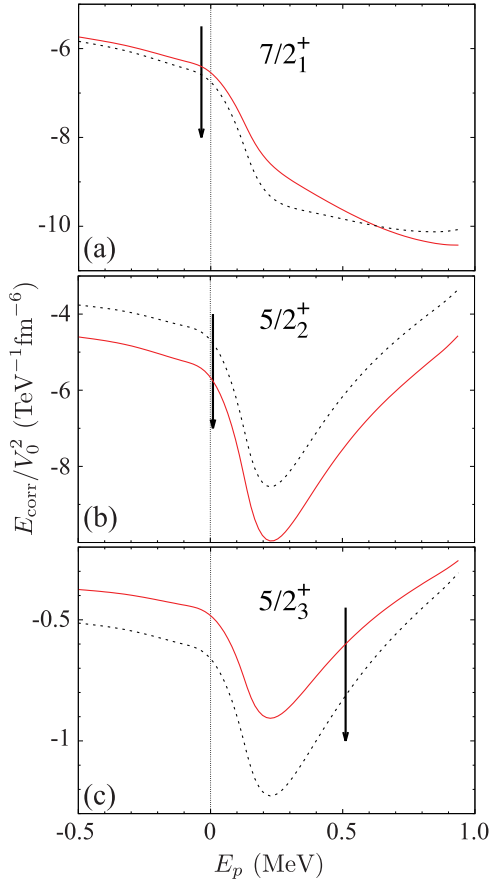
FIG. 2. Real part of the continuum-coupling correlation energy for three near proton-threshold states in ^{11}C: (a) the weakly bound state $7/2_1^+$ state; (b) the resonance state $5/2_2^+$, 10 keV just above the proton emission threshold; and (c) the resonance state $5/2_3^+$. The SMEC results are shown as a function of the proton energy E_p in the continuum. Zero energy corresponds to the proton decay threshold. The arrows denote the experimental resonance energies. The $k = 3$ and $k = 4$ SMEC results are shown by dashed and solid lines, respectively.

a strong coupling between $d_{5/2}$ and $s_{1/2}$ proton channels with different ℓ.

The proton $s_{1/2}$ and $d_{5/2}$ spectroscopic factors of the $7/2_1^+$ state in ^{11}C are listed in Table I for different SM and SMEC calculation variants. The $d_{3/2}$ SM spectroscopic factor is smaller, $\mathcal{S}_{d3/2} \approx 0.065$, and remains practically unchanged in SMEC. There is only a small difference between values

TABLE I. The proton $s_{1/2}$ and $d_{5/2}$ spectroscopic factors $\mathcal{S}_{\ell j}^{(k)}$ of the $7/2_1^+$, $5/2_2^+$, and $5/2_3^+$ resonances in the vicinity of the proton threshold in ^{11}C obtained in different calculation variants.

J^π	$\mathcal{S}_{s1/2}^{(1)}$	$\mathcal{S}_{s1/2}^{(2)}$	$\mathcal{S}_{s1/2}^{(3)}$	$\mathcal{S}_{s1/2}^{(4)}$	$\mathcal{S}_{d5/2}^{(1)}$	$\mathcal{S}_{d5/2}^{(2)}$	$\mathcal{S}_{d5/2}^{(3)}$	$\mathcal{S}_{d5/2}^{(4)}$
	SM		SMEC		SM		SMEC	
$7/2_1^+$	0.15	0.09	0.12	0.10	0.36	0.37	0.34	0.38
$5/2_2^+$	0.29	0.32	0.38	0.33	0.12	0.19	0.19	0.19
$5/2_3^+$	0.08	0.06	0.02	0.04	0.01	0.01	0.04	~ 0

of $\mathcal{S}_{d5/2}$ for different choice of monopoles and between SM and SMEC calculation. For $s_{1/2}$ spectroscopic factor, differences between SM results obtained for different monopoles are larger but they decrease in SMEC.

It should be stressed that our objective is to verify whether one can obtain a reasonable description of $7/2_1^+$, $5/2_2^+$, $5/2_3^+$ resonances in ^{11}C in the SMEC framework using either of these interactions. We have found that the correct order of the considered resonances can be obtained in SMEC ($k = 4$) using the modified version of SM interaction ($k = 2$) with the continuum-coupling strength comparable to the one used in studies of ^{11}B [10,11]. SMEC calculation with the SM interaction of ^{11}B ($k = 1$) gives a correct position of only two resonances for a significantly stronger continuum-coupling interaction strength. The effect of two different relevant interactions and two different many-body approaches can be seen by comparing the proton decay width of $5/2_2^+$ resonance calculated with two SMEC interactions ($k = 3, 4$), and the spectroscopic factors in Table I. Even though the spectroscopic factors are not observables [30–32] and the calculated numbers given in Table I should be viewed as reasonable estimates only, it is worth noting that the SMEC $\mathcal{S}_{s1/2}$ spectroscopic factor of $5/2_2^+$ resonance is close to the experimental spectroscopic factor reported in the direct capture reaction [29].

Figure 2(b) shows $E_{\rm corr}$ for a threshold $5/2_2^+$ resonance. Among all the $5/2^+$ SMEC states calculated, only this resonance has characteristics of the aligned state. One can see that the dependence of $E_{\rm corr}$ on the choice of the monopole terms is stronger than for the $7/2_1^+$ state, but for both calculation variants the continuum-coupling correlation energy is large and the minimum of $E_{\rm corr}(E_{\rm p})$ hardly depends on the choice of the monopole terms. The $5/2_2^+$ state aligns with a channel $[^{10}{\rm B}(3^+) \otimes p(s_{1/2})]^{5/2^+}$ and has a large $s_{1/2}$ spectroscopic factor, which increases when going from SM to SMEC, as expected. The spectroscopic factor $\mathcal{S}_{d5/2}$ is not negligible and $\mathcal{S}_{d3/2}$ is smaller by a factor ≈ 2 as compared to $\mathcal{S}_{d5/2}$. Finally, Fig. 2(c) shows $E_{\rm corr}$ for a near-threshold $5/2_3^+$ resonance. Compared to the $5/2_2^+$ resonance, the continuum-coupling energy correction of this state is reduced by an almost one order of magnitude.

Considering the results presented in Fig. 2 and Table I, we conclude that the low-energy cross section for the reaction $^{10}{\rm B}(p, \alpha)^7{\rm Be}$ is expected to be enhanced by the presence of the threshold resonance $5/2_2^+$, which is strongly coupled to the $\ell = 0$ proton decay channel. The impact of the subthreshold state $7/3_1^+$ is weaker, but not negligible.

Conclusions. Aneutronic energy production in the boron-proton plasma is poisoned by a spurious amounts of radioactive ^{7}Be produced in the reaction $^{10}{\rm B}(p, \alpha)^7{\rm Be}$. The cross section for this reaction at energies accessible by the National Ignition Facility [33] or OMEGA EP [34] laser-driven hot plasma facilities, cannot be measured directly in accelerator based measurements and is usually obtained from the phenomenological R-matrix analysis. As stated in Ref. [35], this approach is questionable for $^{10}{\rm B}(p, \alpha)^7{\rm Be}$ reaction due to insufficient and inconsistent experimental data.

The theoretical SMEC analysis shows that the low-energy proton continuum in ^{11}C is determined mainly by the near-threshold resonance $5/2_2^+$ and, to a lesser extent, the subthreshold level $7/2_1^+$. The calculated spectroscopic factor for the $5/2_2^+$ resonance is in a qualitative agreement with the phenomenological analysis [35]. However, the resonance width predicted in SMEC exceeds by 3 to 4 orders of magnitude the value obtained from extrapolation the low-energy data down to zero energy [3,35].

Even though the $5/2_2^+$ and $7/2_1^+$ resonances decay predominantly by the α-particle emission, their nature is strongly modified by the nearby proton decay threshold. Both states, collectivized by the coupling to reaction channels $[^{10}\mathrm{B}(3^+) \otimes p(s_{1/2})]^{5/2^+, 7/2^+}$, $[^{10}\mathrm{B}(3^+) \otimes p(d_{5/2})]^{5/2^+, 7/2^+}$ are the doorways for the proton capture by ^{10}B. Consequently, the presence of threshold-aligned proton resonances is expected to strongly enhance the $^{10}\mathrm{B}(p, \alpha)^7\mathrm{Be}$ cross section at energies accessible to the laser driven hot plasma facilities.

[1] L. Lamia *et al.*, Boron depletion: Indirect measurement of the ^{10}B(p,α)^{7}Be S(E)-factor, Nucl. Phys. A **787**, 309 (2007).

[2] C. Spitaleri *et al.*, Measurement of the 10 kev resonance in the ^{10}B(p, α_0)^{7}Be reaction via the Trojan Horse method, Phys. Rev. C **90**, 035801 (2014).

[3] C. Spitaleri *et al.*, Measurement of the ^{10}B(p, α_0)^{7}Be cross section from 5 keV to 1.5 MeV in a single experiment using the Trojan horse method, Phys. Rev. C **95**, 035801 (2017).

[4] Michael Wiescher and Tan Ahn, Clusters in Astrophysics, in *Nuclear Particle Correlations and Cluster Physics*, edited by Wolf-Udo Schröder (World Scientific, Singapore, 2017), p. 203.

[5] J. Okołowicz, M. Płoszajczak, and W. Nazarewicz, On the origin of nuclear clustering, Prog. Theor. Phys. Suppl. **196**, 230 (2012).

[6] Y. Ayyad *et al.*, Direct Observation of Proton Emission in ^{11}Be, Phys. Rev. Lett. **123**, 082501 (2019).

[7] Y. Ayyad *et al.*, Evidence of a Near-Threshold Resonance in ^{11}B Relevant to the β-Delayed Proton Emission of ^{11}Be, Phys. Rev. Lett. **129**, 012501 (2022).

[8] E. Lopez-Saavedra *et al.*, Observation of a Near-Threshold Proton Resonance in ^{11}B, Phys. Rev. Lett. **129**, 012502 (2022).

[9] B. V. Kolk, K. T. Macon, R. J. deBoer, T. Anderson, A. Boeltzig, K. Brandenburg, C. R. Brune, Y. Chen, A. M. Clark, T. Danley, B. Frentz, R. Giri, J. Gorres, M. Hall, S. L. Henderson, E. Holmbeck, K. B. Howard, D. Jacobs, J. Lai, Q. Liu, J. Long, K. Manukyan, T. Massey, M. Moran, L. Morales, D. Odell, P. O'Malley, S. N. Paneru, A. Richard, D. Schneider, M. Skulski, N. Sensharma, C. Seymour, G. Seymour, D. Soltesz, S. Strauss, A. Voinov, L. Wustrich, and M. Wiescher, Investigation of the ^{10}B(p, α)^{7}Be reaction from 0.8 to 2.0 MeV, Phys. Rev. C **105**, 055802 (2022).

[10] J. Okołowicz, M. Płoszajczak, and W. Nazarewicz, Convenient Location of a Near-Threshold Proton-Emitting Resonance in ^{11}B, Phys. Rev. Lett. **124**, 042502 (2020).

[11] J Okołowicz, M Płoszajczak, and W Nazarewicz, $\beta^- p$ and $\beta^- \alpha$ decay of the ^{11}Be neutron halo ground state, J. Phys. G: Nucl. Part. Phys. **49**, 10LT01 (2022).

[12] J. Chen *et al.*, Observation of the near-threshold intruder 0^- resonance in ^{12}Be, Phys. Rev. C **103**, L031302 (2021).

[13] R. J. Charity *et al.*, Observation of the Exotic Isotope ^{13}F Located Four Neutrons Beyond the Proton Drip Line, Phys. Rev. Lett. **126**, 132501 (2021).

[14] F. de Grancey *et al.*, An above-barrier narrow resonance in ^{15}F, Phys. Lett. B **758**, 26 (2016).

[15] V. Girard-Alcindor *et al.*, New narrow resonances observed in the unbound nucleus ^{15}F, Phys. Rev. C **105**, L051301 (2022).

[16] R. J. Charity *et al.*, Spin alignment following inelastic scattering of ^{17}Ne, lifetime of ^{16}F, and its constraint on the continuum coupling strength, Phys. Rev. C **97**, 054318 (2018).

[17] R. J. Charity *et al.*, Invariant-mass spectroscopy of ^{14}O excited states, Phys. Rev. C **100**, 064305 (2019).

[18] Y. Kondo *et al.*, Nucleus ^{26}O: A Barely Unbound System Beyond the Drip Line, Phys. Rev. Lett. **116**, 102503 (2016).

[19] F. C. Barker, A model for nuclear threshold levels, Proc. Phys. Soc. **84**, 681 (1964).

[20] J. Okołowicz, M. Płoszajczak, and I. Rotter, Dynamics of quantum systems embedded in a continuum, Phys. Rep. **374**, 271 (2003).

[21] J. Okołowicz, W. Nazarewicz, and M. Płoszajczak, Toward understanding the microscopic origin of nuclear clustering, Fortschr. Phys. **61**, 66 (2013).

[22] B. Jonson and K. Riisager, Beta-decay of exotic nuclei, Nucl. Phys. A **693**, 77 (2001).

[23] D. Baye and E.M. Tursunov, Beta delayed emission of a proton by a one-neutron halo nucleus, Phys. Lett. B **696**, 464 (2011).

[24] M. J. G. Borge, L. M. Fraile, H. O. U. Fynbo, B. Jonson, O. S. Kirsebom, T. Nilsson, G. Nyman, G. Possnert, K. Riisager, and O. Tengblad, Rare βp decays in light nuclei, J. Phys. G: Nucl. Part. Phys. **40**, 035109 (2013).

[25] K. Riisager *et al.*, ^{11}Be(βp), a quasi-free neutron decay? Phys. Lett. B **732**, 305 (2014).

[26] Cen-Xi Yuan, Impact of off-diagonal cross-shell interaction on ^{14}C, Chin. Phys. C **41**, 104102 (2017).

[27] K. Bennaceur, F. Nowacki, J. Okołowicz, and M. Płoszajczak, Analysis of the ^{16}O(p,γ)^{17}F capture reaction using the shell model embedded in the continuum, Nucl. Phys. A **671**, 203 (2000).

[28] National Nuclear Data Center, http://www.nndc.bnl.gov/.

[29] M. Wiescher, R. N. Boyd, S. L. Blatt, L. J. Rybarcyk, J. A. Spizuoco, R. E. Azuma, E. T. H. Clifford, J. D. King, J. Görres, C. Rolfs, and A. Vlieks, ^{11}C level structure via the ^{10}B(p, γ) reaction, Phys. Rev. C **28**, 1431 (1983).

[30] R. J. Furnstahl and H. W. Hammer, Are occupation numbers observables? Phys. Lett. B **531**, 203 (2002).

[31] T. Duguet, H. Hergert, J. D. Holt, and V. Somà, Nonobservable nature of the nuclear shell structure: Meaning, illustrations, and consequences, Phys. Rev. C **92**, 034313 (2015).

[32] M. Gómez-Ramos, A. Obertelli, and Y. L. Sun, Breakup reactions and their ambiguities, Eur. Phys. J. A **57**, 148 (2021).

[33] W.J. Hogan, E.I. Moses, B.E. Warner, M.S. Sorem, and J.M. Soures, The national ignition facility, Nucl. Fusion **41**, 567 (2001).

[34] M. J. Guardalben, M. Barczys, B. E. Kruschwitz, M. Spilatro, L. J. Waxer, and E. M. Hill, Laser-system model for enhanced operational performance and flexibility on OMEGA EP, High Power Laser Sci. Eng. **8**, e8 (2020).

[35] M. Wiescher, R. J. deBoer, J. Görres, and R. E. Azuma, Low energy measurements of the ^{10}B$(p, \alpha)^7$Be reaction, Phys. Rev. C **95**, 044617 (2017).